IEEE
ELECTRON DEVICE LETTERS

MAY 2022 VOLUME 43 NUMBER 5 EDLEDZ (ISSN 0741-3106)

MOSFET on Chemical-Mechanical Planarized Heteroepitaxial Diamond

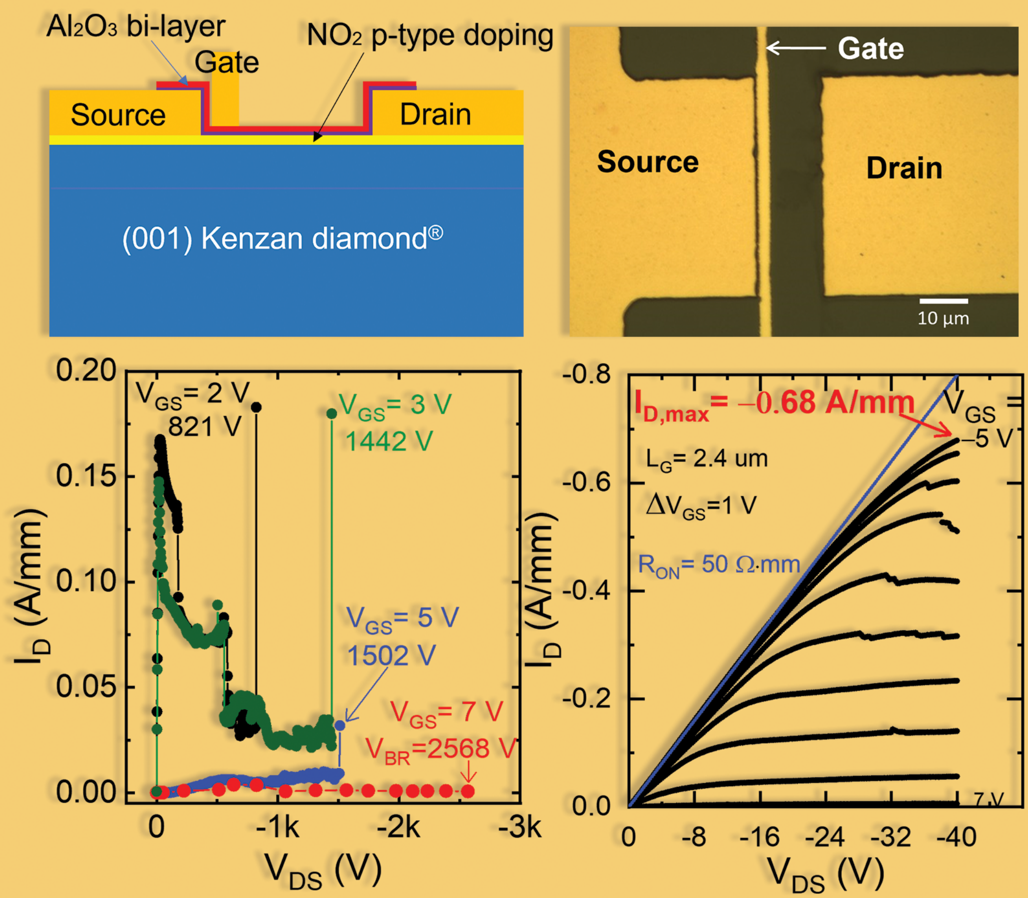

Also in this issue:

- Field-Free Magnetic Switching of Spin-Orbit Torque Magnetic Tunneling Junction
- Flexible Nanocellulose ITO Device With Solid-State Electrolyte
- Thin-Body Ga_2O_3 Schottky Diode
- Teraherz Power Module Based on 0.34 THz Traveling Wave Tube

A PUBLICATION OF THE IEEE ELECTRON DEVICES SOCIETY

875-MW/cm^2 Low-Resistance NO_2 p-Type Doped Chemical Mechanical Planarized Diamond MOSFETs

Niloy Chandra Saha, Seong-Woo Kim, Toshiyuki Oishi, *Senior Member, IEEE*, and Makoto Kasu

***Abstract*—In this study, an Al_2O_3 passivated, NO_2 p-type doped diamond metal–oxide–semiconductor field-effect transistor (MOSFET) was fabricated on a chemical mechanical planarized high-quality heteroepitaxial diamond (Kenzan diamond®) substrate. This MOSFET exhibited a low specific ON-resistance of 7.54 m$\Omega\cdot$cm^2 and a high OFF-state breakdown voltage of −2568 V. The chemical mechanical planarization (CMP) was performed for 200 h on the diamond surface which effectively removed the subsurface damages resulting in a low resistive diamond surface. Thus, the MOSFET showed a high drain current density of −0.68 A/mm and a maximum available power density (Baliga's figure-of-merit) of 874.6 MW/cm^2—the highest reported value for diamond devices.**

***Index Terms*—CMP, diamond MOSFET, heteroepitaxial diamond, high BFOM, NO_2 p-type doping.**

I. Introduction

DIAMOND, with an ultrawide bandgap of 5.47 eV, is the most promising semiconductor material for high-power and high-frequency transistors. It possesses a high breakdown electric field of >10 MV/cm [1], [2] and a thermal conductivity of 22 W/cm·K [3]. Further, undoped diamond exhibits high carrier mobilities (electron and hole mobilities of 4500 and 3800 cm^{2}V^{-1}s^{-1}, respectively) [4]. Hydrogen termination on diamond forms a two-dimensional hole channel, and the hole density and mobility can be controlled by varying the temperature during the hydrogen termination [5]. Hydrogen terminated diamond (H-diamond) field-effect transistors show excellent radiofrequency (RF) characteristics, such as RF power densities of 2.1 and 3.8 W/mm at 1 GHz [6], [7], a maximum cut-off frequency (f_T) of 70 GHz [8], and a maximum oscillation frequency (f_{max}) of 120 GHz [9].

Manuscript received March 22, 2022; accepted March 31, 2022. Date of publication April 4, 2022; date of current version April 26, 2022. This work was supported by the Japan Society for the Promotion of Science (JSPS) Grants-in-aid for Scientific Research under Grant 19H02616. The review of this letter was arranged by Editor B. G. Malm. *(Corresponding author: Makoto Kasu.)*

Niloy Chandra Saha, Toshiyuki Oishi, and Makoto Kasu are with the Department of Electrical and Electronic Engineering, Saga University, Saga 840-8502, Japan (e-mail: sniloy109@gmail.com; kasu@cc.saga-u.ac.jp).

Seong-Woo Kim is with Adamant Namiki Precision Jewel Company, Ltd., Tokyo 123-8511, Japan.

Color versions of one or more figures in this letter are available at https://doi.org/10.1109/LED.2022.3164603.

Digital Object Identifier 10.1109/LED.2022.3164603

NO_2 p-type doping is used in H-diamond to increase the hole carrier concentration (p_s), which can be reportedly increased by one order of magnitude (up to $\sim 2.4 \times 10^{14}$ cm^{-2}) than that in air [10], [11]. An Al_2O_3 layer is used to passivate the hole channel and attain thermal stabilization [12]. Hirama *et al.* [13] demonstrated a diamond metal–oxide–semiconductor field-effect transistor (MOSFET) with the highest drain current density of 1.35 A/mm, using NO_2 doping and an Al_2O_3 layer. Saha *et al.* [14], [15] demonstrated high-drain-current-density and high-breakdown-voltage MOSFETs on heteroepitaxial diamond, which were grown on sapphire substrates using the microneedle technique. One-inch diamond substrates with a low dislocation density (1.4×10^7 cm^{-2}) and high crystallinity (113.4 arcsec) were reported as well [16]. Moreover, freestanding diamond with a diameter of 2″ was demonstrated using a step-flow growth on misoriented sapphire [17]. Heteroepitaxial diamond MOSFETs also exhibited the highest lateral breakdown voltage of −2608 V and a Baliga's figure-of-merit (BFOM) of 345 MW/cm^2 [18].

Mechanical polishing, which induces subsurface damages [19], has been widely used on heteroepitaxially grown diamond substrates to obtain a flat surface. To eliminate the subsurface damages and obtain an atomically flat surface, which is desirable for a smoother carrier transport at the heterointerfaces, chemical mechanical planarization (CMP) is applied [20]. In this study, we fabricated NO_2 p-type doped diamond MOSFETs on heteroepitaxial diamond substrates treated using CMP for 200 h. These MOSFETs exhibited very high drain currents, high mobilities, low ON resistances, and high breakdown voltages, and therefore, a high BFOM.

II. Growth and Fabrication

Fig. 1(a) shows the cross-section of the diamond MOSFET fabricated on an 8.0×8.0 mm^2 high-quality heteroepitaxial (001) diamond freestanding substrate (Kenzan diamond®). The diamond substrate was grown on sapphire using the microneedle technique and then, treated with CMP for 200 h to remove the mechanical polishing-induced subsurface damages. CMP was performed using the abrasive slurry of Cr_2O_3 at a rotating speed of 3.6 m/s and a pressure of 15 kPa. During the 50 and 200 h of CMP, approximately 90- and 360-μm-thick diamond layers were removed, respectively. As the CMP

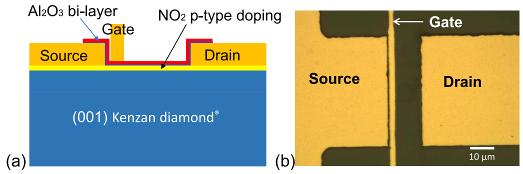

Fig. 1. (a) Schematic of the cross-section and (b) microscopic top view of an NO_2 p-type doped heteroepitaxial diamond (Kenzan diamond®) MOSFET.

progressed, the hidden subsurface damages appeared on the surface, and 200 h of CMP was required to completely remove these damages. The full width at half maximum of the 004 X-ray rocking curve was 259 arcsec, and the surface roughness was 0.04 nm. An approximately 125-nm-thick diamond homoepitaxial layer was grown on the diamond substrate using microwave plasma chemical vapor deposition. During the growth, source gases CH_4 and H_2 were supplied in a ratio of 1:100, and the microwave power and working pressure were 750 W and 50 Torr, respectively.

The NO_2 p-type doping was performed by exposing the H-diamond sample to 2 % NO_2 gas diluted in N_2. To form the ohmic contact, a 50-nm-thick Au layer was deposited on it. The active hole channel was formed by separating the source–drain (S/D) contacts. However, during the S/D fabrication, the active channel was subjected to several processes that reduced the sheet concentration. Thus, the active channel was again exposed to 2 % NO_2 (diluted in N_2).

A 16-nm-thick Al_2O_3 bilayer, which also served as the gate insulating layer, was deposited using the atomic layer deposition method in a high vacuum chamber to passivate the channel without exposing it to air. Trimethylaluminum and H_2O were sequentially supplied as the Al and O sources, respectively. The deposition temperatures of the Al_2O_3 bilayer were 120 °C (first layer: 4-nm thick) and 230 °C (second layer: 12-nm thick), respectively.

Finally, a 50-nm-thick gate (Au layer) was deposited adjacent to the source contact, depicted as the microscopic top view of the diamond MOSFET in Fig. 1(b) [21]. The active channel length (source-to-drain length, L_{SD}), gate length (L_G), and gate width were 13.6, 2.4, and 44.9 μm, respectively. The DC output characteristics of the MOSFETs were measured at 25 °C using the Keysight 1505A power device analyzer and Keithley 248 high voltage supply.

III. Results and Discussion

Fig. 2(a) shows the current-voltage characteristics of two ohmic contacts with a spacing of 13.6 μm at different stages of fabrications. A total resistance (R_T) of 68.5 Ω·mm was determined after the S/D fabrication and a significantly reduced R_T of 38 Ω·mm was measured when the NO_2 doping was performed again at the active channel. It indicates that increased resistance due to the fabrication-related processes can be substantially lowered by the NO_2 p-type doping. However, after the Al_2O_3 bilayer deposition, R_T becomes 53 Ω·mm.

Fig. 2(b) shows the variations in R_T with different contact spacings d (CMP for 200 h). The contact resistance (R_C) and sheet resistance (R_{SH}) were determined using the transfer length method (TLM) performed after the Al_2O_3 bilayer deposition. The R_T values at different d were fitted linearly, yielding $2R_C = 5.24$ Ω·mm as the intercept, $R_{SH} = 3.55$ kΩ/sq as the slope, and a transfer contact length (L_T) of 1.48 μm.

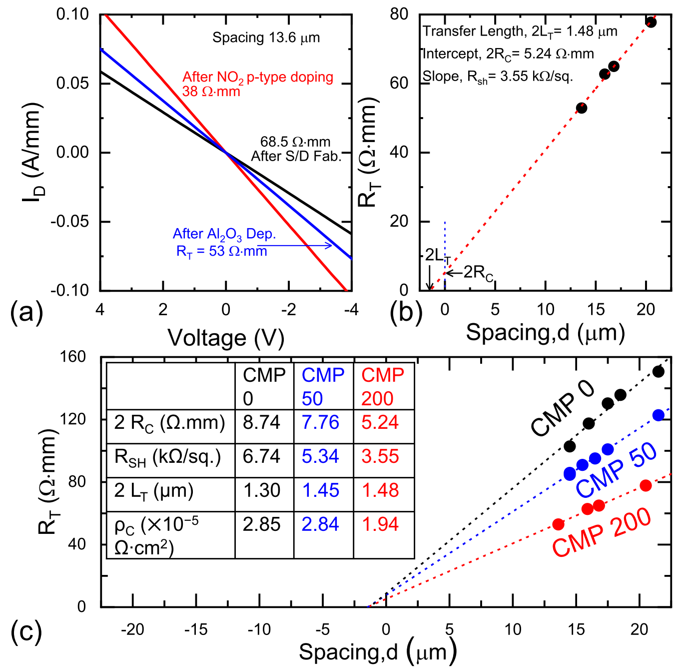

Fig. 2. (a) Current–voltage characteristics of the two ohmic contacts at different stages of fabrication, and (b) R_T as a function of the ohmic contacts spacing, d, after the Al_2O_3 bilayer deposition on the heteroepitaxial diamond (CMP of 200 h). (c) Comparison of the TLM-measured parameters corresponding to diamond substrates with CMP treatment of 0, 50 [14], and 200 h.

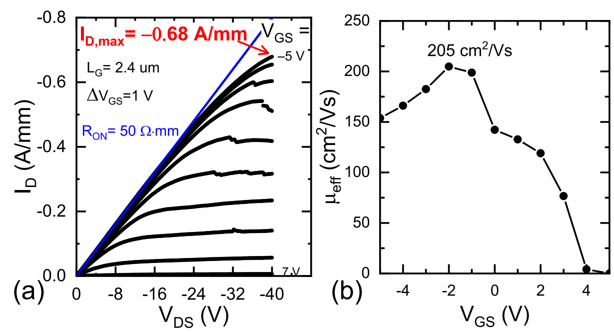

Fig. 3. (a) I_D-V_{DS} and (b) $\mu_{eff}-V_{GS}$ characteristics of the diamond MOSFET with NO_2 p-type doping and an Al_2O_3 passivation layer.

Furthermore, Fig. 2 (c) presents a comparison between the TLM-measured parameters of the CMP-treated diamond substrates with treatment times of 0, 50, and 200 h. Evidently, R_C, R_{SH}, and the contact resistivity (ρ_C) decrease with the increasing treatment time. The lowest ρ_C of 1.94 × 10^{-5} Ω·cm^2 was obtained for the diamond substrates treated for 200 h. Owing to the lower resistive H-diamond surface of 200 h of CMP treated sample has lower R_C and ρ_C. Even the diamond surface roughnesses after the CMP of 0, 50, and 200 h were within the same level, i.e., 0.02, 0.05, and 0.04 nm, respectively. Thus, the effective removal of subsurface damages using CMP results in a highly conductive H-diamond surface.

Fig. 3(a) shows the drain current–voltage (I_D–V_{DS}) characteristics of the diamond MOSFET on the heteroepitaxial

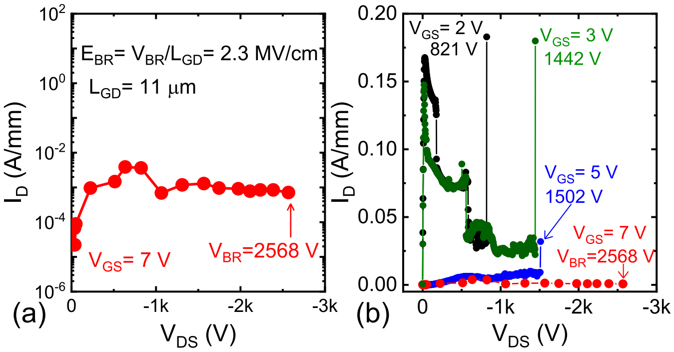

Fig. 4. (a) OFF-state $I_D - V_{DS}$ characteristics of the diamond MOSFETs at $V_{GS} = 7$ V, and (b) ON-state and OFF-state drain current characteristics of the diamond MOSFETs at different V_{GS}.

diamond (200 h of CMP). The maximum I_D was 0.68 A/mm at a gate voltage (V_{GS}) of −7 V and V_{DS} of −40 V. A low ON resistance of 50 Ω·mm was estimated from the linear region of the I_D curve at a V_{GS} of −7 V. The low R_C and R_{SH} enabled the MOSFET to exhibit such a high current and low resistance. The gate leakage current was <1 μA/mm, and the maximum transconductance ($g_{m,max}$ = dI_D/dV_{GS}) was 101 mS/mm at $V_{GS} = -1$ V. The threshold voltage (V_{th}) was 4.1 ± 0.1 V, which was determined by linearly extrapolating the I_D–V_{GS} characteristics at $V_{DS} = -0.2$ V, indicating that the MOSFET exhibits a normal ON operation.

Fig. 3(b) shows the gate-voltage-dependent effective mobility (μ_{eff}–V_{GS}) characteristics. The μ_{eff} values were estimated using (1) below:

$$R_{CH}W_G = \frac{L_G}{\mu_{eff}C_{ox}|V_{GS} - V_{th}|} \quad (1)$$

where R_{CH} is the channel resistance under the gate, and the capacitance of the Al_2O_3 layer, C_{OX}, is 343 nF/cm^2 (determined by measuring the capacitance of the metal–insulator–metal structure). The R_{CH} values were obtained using the equation, $R_{CH} = R_{ON} - 2R_C - R_{SH}$ ($L_{SD} - L_G$), and a maximum μ_{eff} of 205 cm^2/Vs was estimated.

Fig. 4(a) shows the OFF-state drain current characteristics of the MOSFET at $V_{GS} = 7$ V, indicating a high breakdown voltage, V_{BR}, of −2568 V. Further increase in the drain voltage produces irreversible damage to the devices. The current flowing through the gate edge on the drain side to the diamond is responsible for the OFF-state drain leakage current. The lateral breakdown field, E_{BR} (= V_{BR}/L_{GD}) was estimated to be 2.3 MV/cm. The gate-to-drain length, $L_{GD}$was 11 μm. Although this E_{BR} is comparable to that of GaN or SiC, it is still much lower than the theoretical value for diamond.

Fig. 4(b) shows a comparison between the ON-state and OFF-state I_D–V_{DS} characteristics at different gate biases. The ON-state breakdown voltages were −821 and −1442 V at a V_{GS} of 2 and 3 V, respectively, and the ON-state currents were started to decrease when V_{DS} reached −40 V. Hot carrier injection into the Al_2O_3 layer degrades the drain current at higher drain voltages. In contrast, the breakdown voltage of −1502 V, obtained at $V_{GS} = 5$ V, can be considered as the OFF-state, because the V_{th} was 4.1 V. A higher drain leakage current flowed from the gate edge to the diamond when V_{DS} reached −180 V. For $V_{GS} = 7$ V, no further increase in the drain current was observed, which enabled the MOSFET to exhibit a high drain voltage of −2568 V.

The MOSFET possessed an active area consisted of L_{SD} and $2L_T$. The specific ON-resistance, $R_{ON,spec}$, was determined to be 7.54 mΩ·cm^2, and consequently, the BFOM was obtained as 874.6 MW/cm^2 using the equation, BFOM = $V_{BR}^2/R_{ON,spec}$, where V_{BR}, L_{SD}, and $2L_T$ were −2568 V, 13.6 μm, and 1.48 μm, respectively. This BFOM value is the highest value ever reported for diamond devices. Further, this BFOM exceeds our previously reported values, because the MOSFETs prepared on the heteroepitaxial diamond substrates, which were treated using CMP for 200 h, exhibited exceptionally low resistances. Among the lateral devices, GaN high electron mobility transistors demonstrated a high-power operation, with a maximum BFOM (to the best of our knowledge) of 2093 MW/cm^2 [22], however, our devices feature a BFOM of approximately 40 % of this value.

IV. Conclusion

In this study, we fabricated diamond MOSFETs using NO_2 p-type doping and an Al_2O_3 bilayer on a heteroepitaxial diamond treated using CMP for 200 h. The TLM measurements showed a low R_C and R_{SH} of 2.62 Ω·mm and 3.55 kΩ/sq, respectively. The maximum I_D of −0.68 A/mm was measured for a MOSFET with $L_G = 2.4$ μm and $L_{SD} = 13.6$ μm. The R_{ON} and μ_{eff} were determined as 50 Ω.mm and 205 cm^2/Vs, respectively. The MOSFET exhibited a high breakdown voltage of −2568 V, and $R_{ON,spec}$ was estimated as 7.54 mΩ·cm^2. Consequently, the highest BFOM of 874.6 MW/cm^2 was experimentally determined, indicating that CMP treatment eliminates the subsurface damages, and therefore, improves the MOSFET characteristics.

References

[1] M. W. Geis, "Growth of device-quality homoepitaxial diamond thin films," *MRS Proc.*, vol. 162, pp. 15–22, Jan. 1989, doi: 10.1557/PROC-162-15.

[2] C. J. Wort and R. S. Balmer, "Diamond as an electronic material," *Mater. Today*, vol. 11, nos. 1–2, pp. 22–28, Jan. 2008, doi: 10.1016/S1369-7021(07)70349-8.

[3] Y. Yamamoto, T. Imai, K. Tanabe, T. Tsuno, Y. Kumazawa, and N. Fujimori, "The measurement of thermal properties of diamond," *Diamond Rel. Mater.*, vol. 6, no. 8, pp. 1057–1061, May 1997, doi: 10.1016/S0925-9635(96)00772-8.

[4] J. Isberg, J. Hammersberg, E. Johansson, T. Wikström, D. J. Twitchen, A. J. Whitehead, S. E. Coe, and G. A. Scarsbrook, "High carrier mobility in single-crystal plasma-deposited diamond," *Science*, vol. 297, pp. 1670–1672, Sep. 2002, doi: 10.1126/science.1074374.

[5] M. W. Geis, M. A. Hollis, G. W. Turner, J. Daulton, J. O. Varghese, K. Klyukin, J. Wang, B. Yildiz, and B. Zhang, "Controlling the carrier density of surface conductive diamond," *Diamond Rel. Mater.*, vol. 122, Feb. 2022, Art. no. 108775, doi: 10.1016/j.diamond.2021.108775.

[6] M. Kasu, K. Ueda, H. Ye, Y. Yamauchi, S. Sasaki, and T. Makimoto, "2 W/mm output power density at 1 GHz for diamond FETs," *Electron. Lett.*, vol. 41, no. 22, p. 1249, 2005, doi: 10.1049/el:20053194.

[7] S. Imanishi, K. Horikawa, N. Oi, S. Okubo, T. Kageura, A. Hiraiwa, and H. Kawarada, "3.8 W/mm RF power density for ALD Al_2O_3-based two-dimensional hole gas diamond MOSFET operating at saturation velocity," *IEEE Electron Device Lett.*, vol. 40, no. 2, pp. 279–282, Feb. 2019, doi: 10.1109/led.2018.2886596.

[8] X. Yu, J. Zhou, C. Qi, Z. Cao, Y. Kong, and T. Chen, "A high frequency hydrogen-terminated diamond MISFET with f_T/f_{max} of 70/80 GHz," *IEEE Electron Device Lett.*, vol. 39, no. 9, pp. 1373–1376, Sep. 2018, doi: 10.1109/LED.2018.2862158.

[9] K. Ueda, M. Kasu, Y. Yamauchi, T. Makimoto, M. Schwitters, D. Twitchen, G. Scarsbrook, and S. Coe, "Diamond FET using high-quality polycrystalline diamond with f_T of 45 GHz and f_{max} of 120 GHz," *IEEE Electron Dev. Lett.*, vol. 27, no. 7, pp. 570–572, Aug. 2006, doi: 10.1109/LED.2006.876325.

[10] M. Kubovic, M. Kasu, H. Kageshima, and F. Maeda, "Electronic and surface properties of H-terminated diamond surface affected by NO_2 gas," *Diamond Rel. Mater.*, vol. 19, nos. 7–9, pp. 889–893, Jul. 2010, doi: 10.1016/j.diamond.2010.02.021.

[11] T. Wade, M. W. Geis, T. H. Fedynyshyn, S. A. Vitale, J. O. Varghese, D. M. Lennon, T. A. Grotjohn, R. J. Nemanich, and M. A. Hollis, "Effect of surface roughness and H-termination chemistry on diamond's semiconducting surface conductance," *Diamond Rel. Mater.*, vol. 76, pp. 79–85, Jun. 2017, doi: 10.1016/j.diamond.2017.04.012.

[12] M. Kasu, H. Sato, and K. Hirama, "Thermal stabilization of hole channel on H-terminated diamond surface by using atomic-layer-deposited Al_2O_3 overlayer and its electric properties," *Appl. Phys. Exp.*, vol. 5, no. 2, Feb. 2012, Art. no. 025701, doi: 10.1143/apex.5.025701.

[13] K. Hirama, H. Sato, Y. Harada, H. Yamamoto, and M. Kasu, "Diamond field-effect transistors with 1.3 A/mm drain current density by Al_2O_3 passivation layer," *Jpn. J. Appl. Phys.*, vol. 51, no. 9R, Sep. 2012, Art. no. 090112, doi: 10.7567/jjap.51.090112.

[14] N. C. Saha, T. Oishi, S. Kim, Y. Kawamata, K. Koyama, and M. Kasu, "145-MW/cm^2 heteroepitaxial diamond MOSFETs with NO_2 p-type doping and an Al_2O_3 passivation layer," *IEEE Electron Device Lett.*, vol. 41, no. 7, pp. 1066–1069, Jul. 2020, doi: 10.1109/LED.2020.2997897.

[15] M. Kasu, N. C. Saha, T. Oishi, and S.-W. Kim, "Fabrication of diamond modulation-doped FETs by NO_2 delta doping in an Al_2O_3 gate layer," *Appl. Phys. Exp.*, vol. 14, no. 5, Apr. 2021, Art. no. 051004, doi: 10.35848/1882-0786/abf445.

[16] S.-W. Kim, Y. Kawamata, R. Takaya, K. Koyama, and M. Kasu, "Growth of high-quality one-inch free-standing heteroepitaxial (001) diamond on (11 $\bar{2}$0) sapphire substrate," *Appl. Phys. Lett.*, vol. 117, no. 20, Nov. 2020, Art. no. 202102, doi: 10.1063/5.0024070.

[17] S.-W. Kim, R. Takaya, S. Hirano, and M. Kasu, "Two-inch high-quality (001) diamond heteroepitaxial growth on sapphire (11$\bar{2}$0) misoriented substrate by step-flow mode," *Appl. Phys. Exp.*, vol. 14, no. 11, Oct. 2021, Art. no. 115501, doi: 10.35848/1882-0786/ac28e7.

[18] N. C. Saha, S.-W. Kim, T. Oishi, Y. Kawamata, K. Koyama, and M. Kasu, "345-MW/cm^2 2608-V NO_2 p-type doped diamond MOSFETs with an Al_2O_3 passivation overlayer on heteroepitaxial diamond," *IEEE Electron Device Lett.*, vol. 42, no. 6, pp. 903–906, Jun. 2021, doi: 10.1109/led.2021.3075687.

[19] H. Aida, H. Takeda, K. Koyama, H. Katakura, K. Sunakawa, and T. Doi, "Chemical mechanical polishing of gallium nitride with colloidal silica," *J. Electrochemical Soc.*, vol. 158, no. 12, 2011, Art. no. H1206, doi: 10.1149/2.024112jes.

[20] K. Koyama, N. Fujita, S.-W. Kim, and M. Yoshimoto, "Removal of mechanical polishing-induced nanoscale damage in diamond by chemical mechanical polishing (CMP)," presented at the MRS Spring Meeting, Apr. 2021.

[21] N. C. Saha and M. Kasu, "Improvement of the Al_2O_3/NO_2/H-diamond MOS FET by using Au gate metal and its analysis," *Diamond Rel. Mater.*, vol. 92, pp. 81–85, Feb. 2019, doi: 10.1016/j.diamond.2018.12.017.

[22] H.-S. Lee, D. Piedra, M. Sun, X. Gao, S. Guo, and T. Palacios, "3000-V 4.3-m$\Omega \cdot$ cm^2 InAlN/GaN MOSHEMTs with AlGaN back barrier," *IEEE Electron Device Lett.*, vol. 33, no. 7, pp. 982–984, Jul. 2012, doi: 10.1109/LED.2012.2196673.